J Fluoresc (2011) 21:1467–1478
DOI 10.1007/s10895-011-0832-4

ORIGINAL PAPER

Cucurbit[7]uril Disrupts Aggregate Formation Between Rhodamine B Dyes Covalently Attached to Glass Substrates

Ronald L. Halterman · Jason L. Moore · Wai Tak Yip

Received: 23 August 2010 / Accepted: 4 January 2011 / Published online: 28 January 2011

Abstract Dye aggregation is detrimental to the performance of high optical density dye-doped photonic materials. To overcome this challenge, the ability of cucurbit[7]uril (CB7) as a molecular host to disrupt aggregate formation on glass substrates was examined. Rhodamine B was covalently attached to glass slides by initially coating the surface with azidohexylsiloxane followed by copper-catalyzed "click" triazole formation with rhodamine B propargyl ester. The absorption and emission spectra of rhodamine B coated slides in water indicated diverse heterogeneous properties as surface dye density varied. Fluorescence quenching due to dye aggregation was evident at high surface dye density. Addition of aqueous cucurbit[7]uril (CB7) to the surface-tethered dyes perturbed the spectra to reveal a considerable reduction in heterogeneity, which suggested that the presence of a surface in close proximity does not significantly impair CB7's ability to complex with tethered rhodamine B.

Keywords Cucurbit[7]uril · CB7 · Rhodamine B · Aggregates · Absorption · Fluorescence

Introduction

Interest in multichromophoric systems has intensified as a result of their application in advanced photonic devices including dye sensitized solar cells [1, 2] and multichromophoric artificial light harvesting systems [3, 4] as well as fluorescent tags for biological molecules [5-7]. Xanthene dyes, particularly the rhodamine family, are commonly used as stand-alone fluorescent probes or reporter tags for biological molecules [8, 9]. Rhodamine dyes are known for their moderate photostability, making them prime candidates for the fabrication of multichromophoric materials. Unfortunately, rhodamine dyes often undergo nonspecific aggregation even in mildly concentrated solutions [10, 11], which posts a major challenge to rhodamine-based optical materials in overcoming the detrimental effects of dye aggregation. As our interest lies in developing long-lasting, high optical density materials for light harvesting antenna applications, new strategies to control interactions between rhodamine dyes packed in close proximity are urgently needed [12, 13].

Prior dye aggregation studies were for the most part performed in solution [11, 14] and focused on the effects of solvent polarity or on donor-acceptor systems with synthetically fixed spatial orientation [15-17]. Some studies on the development of advanced photonic materials have focused on organizing chromophores on solid substrates [18, 19] or encapsulating chromophores randomly inside solid matrices to enhance photostability. For example, rhodamine 6G (R6G) has been reported to exhibit higher photostability when trapped inside a silica sol-gel monolith [20]. A common problem to these methods is the freedom of the dye molecules to aggregate prior to encapsulation. In the case of rhodamine dyes, the lowest energy dimer is a non-emissive H-type aggregate with two parallel xanthene planes stacking at a head-to-tail orientation with respect to the heteroatom [21, 22]. This H-type aggregate will dramatically reduce the quantum efficiency of the aggregate and thus compromise the performance of a photonic material. Interestingly, it has been shown that H-type aggregate formation can be prevented by imposing steric

R. L. Halterman (✉) · J. L. Moore · W. T. Yip (✉)
Department of Chemistry and Biochemistry,
101 Stephenson Parkway, University of Oklahoma,
Norman, OK 73019, USA
e-mail: RHalterman@ou.edu

W. T. Yip
e-mail: ivan-yip@ou.edu

effects either through the use of short or rigid tethering linkers in rhodamine dyads [8] or through complexation with bulky ligands [23].

In our previous work we had established that aqueous solutions of covalently tethered rhodamine B dimers with long tethers are flexible enough to adopt a head-to-tail H-type dimer conformation [23]. These dimers exhibited shifted absorption maxima and diminished fluoresence intensity as compared to monomeric rhodamine B (RhB). Addition of CB7, a cyclic heptamer of glycolurea/formaldehdye known to bind very strongly to many cationic guests [24-26], disrupted aggregation and increased fluorescence [23]. Given the desirable effects of CB7 to increase the photostability of rhodamine dyes in solution [8] and to enhance the fluorescence of tethered dimers, we next wanted to determine whether the same effect can be observed in densely packed surface attached rhodamine dyes. While it has been demonstrated that CB7 can form very stable complexes with R6G in free solution, it is unclear whether a rhodamine dye covalently attached onto a silica substrate is flexible enough to produce a stable complex with CB7. Of particular interest is to examine whether the mostly negatively charged silica surface may adversely impact the affinity of CB7 toward surface attached cationic rhodamine dyes. When designing photovoltaic materials that based on multichromophoric light harvesting approach, sensitizer-like organic dyes are usually packed in close proximity at the solid-air interfaces. Aggregation between organic dyes becomes a real possibility, which may dramatically reduce the light harvesting efficiency of the materials. If CB7 can complex with surface attached rhodamine dyes, not only can it reduce the propensity of dye aggregation to preserve light harvesting efficiency, it may also increase the photostability of the complexing dyes and prolong the usable lifetime of the photovoltaic devices.

In this work, RhB is attached to the surface of a glass substrate to examine its interactions with CB7. Surface attached RhB were examined at various surface densities in order to assess the effect of RhB aggregation on its optical properties. By monitoring the changes in RhB's optical properties upon CB7 addition, we were able to determine whether CB7 is capable of maintaining its strong affinity of RhB even in the presence of a silica surface nearby, thus disrupting aggregate formation and paving the way to producing high optical density dye-doped photonic materials.

Methods

Choice of Surface Attachment Chemistry

Although dyes with reactive groups had been routinely attached to amino-functionalized solid substrates [27, 28], we choose to avoid this well-established approach for fear that a protonated amino group may attract unwanted Coulombic interactions toward CB7. It has been shown that CB7 has a strong affinity toward ammonium [29] and pyridinium [30-32] ions. The possibility that these ions can be present in the attachment linker may significantly affect the interactions between CB7 and surface attached RhB. Instead we were attracted to Collman's approach that utilizes azido as the functional group to afford RhB attachment to eliminate the possibility of ammonium ion formation [33]. In this approach, we employed a two-stage technique to attach RhB dyes to glass surface by initially forming a mixed 6-azidohexylsilane/hexylsilane-derived adlayer with varying density of azido functionality. RhB attachment was subsequently accomplished through a copper catalyzed cycloaddition by presenting the azido glass to RhB propargyl ester. The control over the density of azido should enable the controlling of surface attached RhB density. The effect of CB7 interaction on RhB at various loading densities could provide crucial information of the ability to control host-guest interactions to yield advantageous optical properties of the complexing dyes.

Preparation of Surface Attached Rhodamine B Ester

At the core of our approach to control the density of surface attached RhB dyes is the initial formation of a mixed adlayer of 6-azidohexylsilane/hexylsilane on glass surfaces. Our strategy was based on the low polarity and minimal differences in non-bonded attraction of the 6-azido-group in the matrix of hexylsilane diluent that would allow an even dispersion of the reactive group in the adlayer. An alternative approach that directly introduced polar RhB with a propensity to aggregate within a growing adlayer seemed more likely to lead to less uniform dispersion of the dyes across the surface. Likewise, the introduction of more polar reactive groups such as an amino group seemed more likely to lead to local clumping of these hydrogen-bonding head groups. Once the desired density of reactive azido groups had been introduced, we could rapidly derivatize the surface with a high concentration of RhB proparyl ester (RhBPE) in the presence of a copper catalyst.

The preparation of dye-modified glass slides is shown in Scheme 1. Hydrosilylation of 6-bromo-1-hexene with triethoxysilane using the Karstedt platinum catalyst gave the known bifunctional 6-bromohexyltriethoxysilane which could be converted with sodium azide in DMSO into 6-azidohexyltriethoxysilane **1** [34]. NMR spectra of crude "N3-C6-Si" **1** indicated that it was pure enough for attachment to the solid glass substrate. We also prepared a complementary acetylenic derivative of RhB for later

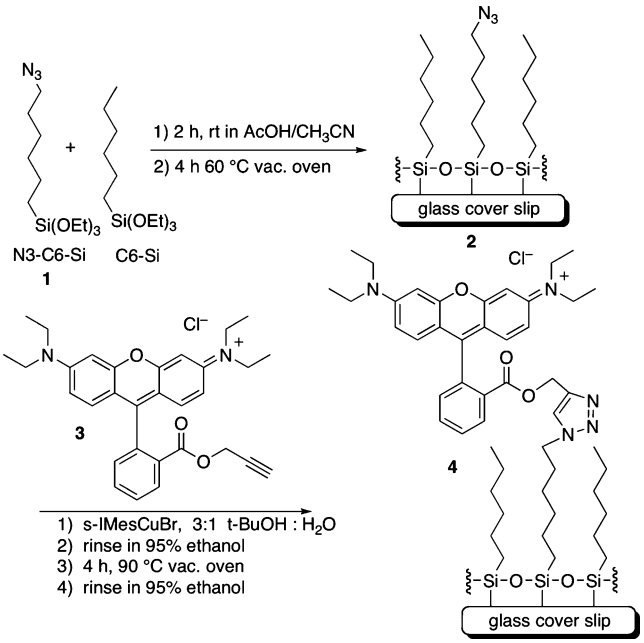

Scheme 1 Preparation of surface-tethered dyes

coupling with the tethered azido groups. RhBPE **3** was prepared from RhB by esterification with propargyl alcohol in the presence of 1,3-dicyclohexylcarbodiimide (DCC) and a catalytic amount of 4-dimethylaminopyridine (DMAP) [35].

In order to control the density of the tethering azido group in the glass coating layer, we exposed glass slides to various mixtures of N3-C6-Si **1** and hexyltriethoxysilane (C6-Si). The total silane concentration was maintained at 10 mM in dry acetonitrile and the ratios varied from 1:1, 1:10, and 1:100 of N3-C6-Si:C6-Si and 100% C6-Si as a control. Piranha-cleaned glass slides [36] were immersed in the silane solutions containing glacial acetic acid [37]. After 2 h at room temperature the slides were removed, transferred to clean tubes without rinsing and pre-cured in a vacuum oven at 60 °C to promote crosslinking [37, 38]. We chose 60 °C to minimize thermal degradation of the terminal azido functionality. This initial curing step was vital since only trace dye signal was measured (*vide infra*) without this step or when the slides were rinsed prior to pre-curing. It appeared that without pre-curing first, the oligomeric siloxane layer was not sufficiently cross-linked to achieve the needed structural stability to withstand subsequent processing required to complete RhB surface attachment.

After pre-curing, a 1,2,3-triazole forming "click" reaction was used to covalently attach RhBPE **3** to the exposed azido head groups [33, 39, 40]. Carrying out the Cu-alkyne-azide-cycloaddition (Cu-AAC) with the common copper iodide/sodium ascorbate system gave unsatisfactory yields in initial reactions. Since we had access to Nolan's single component sIMesCuBr catalyst for use in Cu-AAC reactions on gold monolayers, we screened its use in this reaction and found it in our hands to give superior results. We did not attempt to optimize the standard copper iodide/sodium ascorbate conditions in favor of using the single component Nolan catalyst. We found that the use of Nolan's sIMesCuBr catalyst gave better results than the more common Cu^{II}/sodium ascorbate system [41]. The N3-C6-Si/C6-Si functionalized slides were immersed in a mixture of *tert*-butyl alcohol and water containing RhBPE **3** and sIMesCuBr (10 mol%) for 8 h at room temperature in the dark. The treated slides were rinsed, dried by centrifugation, cured in a vacuum oven at 90 °C for 4 h to promote further crosslinking, rinsed again and soaked overnight in 1:1 water:ethanol to remove all non-tethered dyes. As the relatively large RhB molecules become surface-attached, access to some densely packed neighboring azido groups may be blocked. Thus not all azido head groups are available for RhB attachment, even though the surface may appear to be saturated with RhB aggregates. At low azido head group coverage, however, it is expected that isolated, non-aggregated surface-attached RhB should predominate.

Results and Discussion

Surface Attached RhBPE Forms Inhomogeneous Aggregates

Absorption and emission spectra of dye-treated slides were measured initially in water and then with added CB7. In Fig. 1, lines A–C show smoothed and baseline corrected absorption spectra in water for dyes attached to a decreasing amount of N3-C6-Si in C6-Si on the glass surface. In each case a maximum signal near 560 nm was observed, which is slightly red-shifted from the 558 nm of the RhBPE solution. As expected, the lowest 1:100 ratio of N3-C6-Si:C6-Si led to a clearly lower absorbance (line C), indicating a lower loading of dye onto the surface. The controls for non-specific adsorption (lines D and E) and when no dye was introduced (line F) gave no discernable absorbance. In addition, samples with higher azido coverage gave similar, but higher absorbance. However, the increase in absorbance appeared not in proportion to the increasing N3-C6-Si:C6-Si ratio. For example, the absorbance from the 1:10 sample is only ~2-fold higher than that of the 1:100 sample, considerably lower than the 10-fold increase expected on the basis of the higher N3-C6-Si concentration used. Since a large excess of RhBPE was used for surface attachment to exhaust all available azido groups, the lower than expected absorbance observed at higher azido coverage might have been the result of steric

hindrance from surface-attached RhB that render some nearby azido groups inaccessible for the "Click" reaction. This effect appears to be even more pronounced in the 1:1 sample, which only registers ~3-fold increase in absorbance over the 1:100 sample.

It is noted that the absorption spectra of the covalently attached dyes on the glass slides were stable even after repeated sonication, indicating that both RhBPE and the siloxane layer are firmly attached onto the glass surface. Although aggregate formation will decrease monomeric RhB absorbance as well, the low absorbance signal from the very thin RhB adlayer precludes us from confidently identifying spectral features that support the presence of RhB aggregates. Aside from the overall 2 nm shift to longer wavelength, the normalized absorption spectra in Fig. 1 inset show no conclusive evidence of either blue- or red-shifted absorbance from H- and J-type dimer, respectively. Nevertheless the inset does show that all RhB adlayer spectra appear to be slightly broader than the RhBPE solution spectrum, which may be due to a combination of both inhomogeneous RhB monomer environment and inhomogeneous RhB aggregate formation. In the latter case, an inhomogeneous aggregate distribution would produce broad and less prominent aggregate absorbance, making it difficult to identify their presence from the absorption spectrum alone.

CB7 Has Strong Affinity Toward Free Rhodamine Dyes in Solution

Our previous work has shown that RhB ethyl ester (RhBEE) has a strong affinity toward CB7, with $K_a = 3 \times 10^6\,\mathrm{M}^{-1}$ based on a non-linear regression analysis of peak intensity at a single wavelength [23]. The emission spectra of 5 μM RhBEE in water and in the presence of CB7 show only strong emission bands near 580 nm (Fig. 2), which indicates the absence of aggregate formation [19, 42]. Here we reanalyzed RhBEE/CB7 binding based on the integration of total emission peak intensity as a function of increasing CB7 concentration.

Assuming that RhBEE and CB7 form a 1:1 complex in solution, the fluorescence intensity (I), integrated from 520 nm to 700 nm, can be fit by Eq. 1.

$$I = \frac{\left(c_0^{\mathrm{RhB}} - c^{\mathrm{RhB/CB7}}\right)}{c_0^{\mathrm{RhB}}} I_0 + \frac{c^{\mathrm{RhB/CB7}}}{c_0^{\mathrm{RhB}}} I_\infty \tag{1}$$

Where c_0^{RhB} and $c^{\mathrm{RhB/CB7}}$ are respectively the initial concentration of RhBEE and the concentration of RhBEE/CB7 complex at different CB7 concentrations. I_0 and I_∞ are fitting parameters representing the fluorescence intensity of RhBEE and RhBEE/CB7, respectively. In this fitting procedure, $c^{\mathrm{RhB/CB7}}$ is calculated according to the equilibrium equation shown in Eq. 2.

$$K_a = \frac{c^{\mathrm{RhB/CB7}}}{c^{\mathrm{RhB}} \cdot c^{\mathrm{CB7}}} = \frac{c^{\mathrm{RhB/CB7}}}{\left(c_0^{\mathrm{RhB}} - c^{\mathrm{RhB/CB7}}\right) \cdot \left(c_0^{\mathrm{CB7}} - c^{\mathrm{RhB/CB7}}\right)} \tag{2}$$

Where c_0^{CB7} is the concentration of CB7 used in recording various emission spectra. Fitting to the data is illustrated in the inset of Fig. 2, which yields $K_a = 5.14 \times 10^5\,\mathrm{M}^{-1}$, I_0=78.3, and I_∞=199.6. The K_a for RhBEE/CB7 determined here is somewhat lower than that determined from single wavelength intensity (3×10^6 M^{-1}) [23]. We can also determine from I_∞/I_0 that the fluorescence enhancement factor for RhBEE upon CB7 binding is about 2.5, which is very close to the ~2.2 fold enhancement found in R6G/CB7 we observed in an earlier investigation [12]. We also note the absence of any spectral shift in $\lambda_{\max}^{\mathrm{em}}$ upon CB7 binding. Assuming that negligible dimer formation occurs at 5 μM RhBEE concentration, the constancy of $\lambda_{\max}^{\mathrm{em}}$ at 581.2±

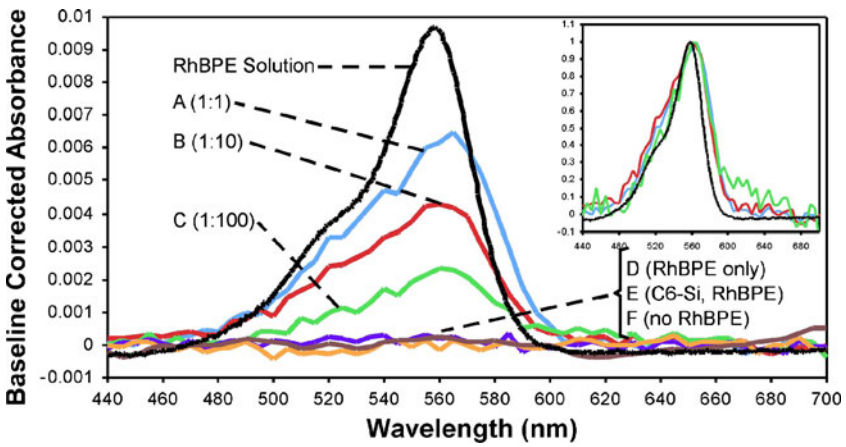

Fig. 1 UV-Vis absorbance spectra of glass slides in water. (**A**) 1:1 N3-C6-Si: C6-Si and RhBPE; (**B**) 1:10 N3-C6-Si: C6-Si and RhBPE; (**C**) 1: 100 N3-C6-Si: C6-Si and RhBPE; **(D)** no silane, RhBPE only; **(E)** C6-Si and RhBPE; **(F)** 1:5 N3-C6-Si: C6-Si, no RhBPE. Inset is the normalized absorption spectra of sample A, B, C, and RhBPE solution

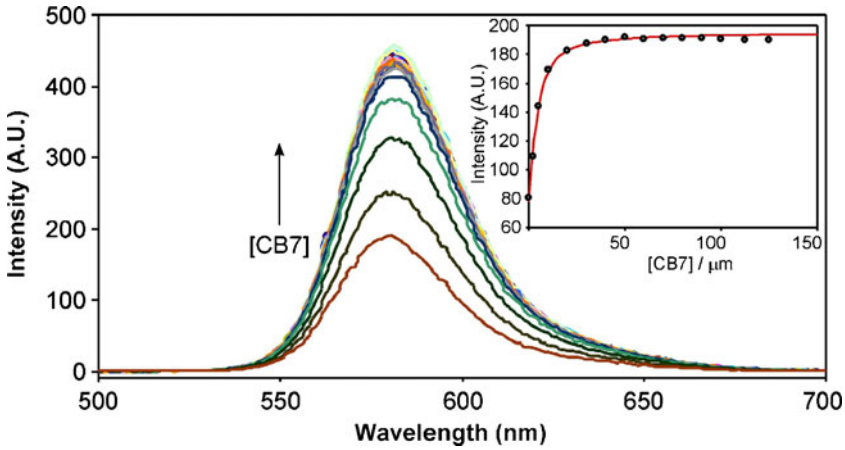

Fig. 2 Fluorescence spectra of RhBEE binding to CB7 as the concentration of CB7 increases from 0 to 5 mM. Inset is the fitting to integrated intensity of the emission spectra as a function of the concentration of CB7 used. All spectra were collected with 5 μM RhBEE (excitation at 530 nm)

0.8 nm suggests that fluorescence enhancement is the only effect of CB7 on RhBEE monomer.

Fluorescence Spectrum Confirms Aggregate Formation in Surface Attached RhB

Despite anticipated strong binding based on previous solution studies, addition of 1 mM CB7 to surface attached RhB at various packing densities did not cause any noticeable change to their respective absorption spectra (Fig. 3). This suggests that either CB7 is incapable of binding to surface-attached RhB or the electronic structure of the immobilized RhB is not significantly altered in a CB7/RhB complex. Although the absorption spectra of RhB were not sensitive enough to differentiate between the two cases, emission spectra from the corresponding samples do provide solid evidence of strong interaction between CB7 and surface attached RhB. The fluorescence spectra of RhB-tethered glass slides in water are shown in Fig. 4. All data were collected using 530 nm excitation in order to minimize the impact of scattered excitation on the emission spectra.

In contrast to the absorption spectra, dramatic changes in both emission intensity and λ_{max}^{em} are noticeable in the fluorescence spectra as azido loading is varied. At the lowest azido loading 1:100 N3-C6-Si:C6-Si sample (line C, λ_{max}^{em} near 580 nm), we noted that the emission spectrum closely resemble the spectra of free RhBEE monomers except for some noticeable broadening at shorter wavelengths [14, 23]. This broadening is most likely due to fluorescence from H-type RhB aggregates as blue-shifted H-type aggregate fluorescence can be caused by direct aggregate excitation at 530 nm or rapid energy transfer from vibronically excited RhB monomers to nearby H-type aggregates. This explanation is further substantiated by a much bigger blue shift observed from the highest azido loading sample (line A for 1:1), where a 10 nm blue-shifted λ_{max}^{em} is registered. Presumably, higher RhB surface density favors aggregate formation and the spectrum becomes dominated by aggregate emission. Relative to the 1:1 sample, the more diluted 1:10 sample produced a slightly less blue-shifted emission. Its resemblance to the emission spectrum of the 1:1 sample more than the 1:100 sample nevertheless suggests that aggregate formation is still

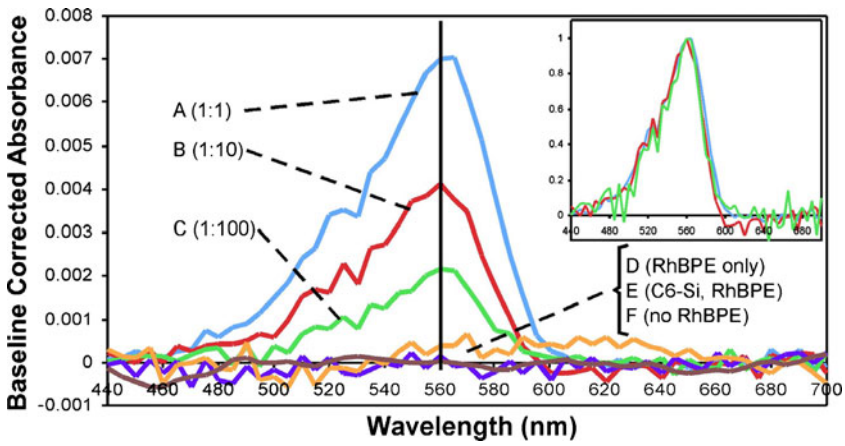

Fig. 3 UV-Vis absorbance spectra of glass slides in 1 mM aqueous solution of CB7. **(A)** 1:1 N3-C6-Si: C6-Si and RhBPE; **(B)** 1:10 N3-C6-Si: C6-Si and RhBPE; **(C)** 1: 100 N3-C6-Si: C6-Si and RhBPE; **(D)** no silane, RhBPE only; **(E)** C6-Si and RhBPE; **(F)** 1:5 N3-C6-Si: C6-Si, no RhBPE. Inset: Normalized spectra of the 1:1, 1:10, and 1:100 samples

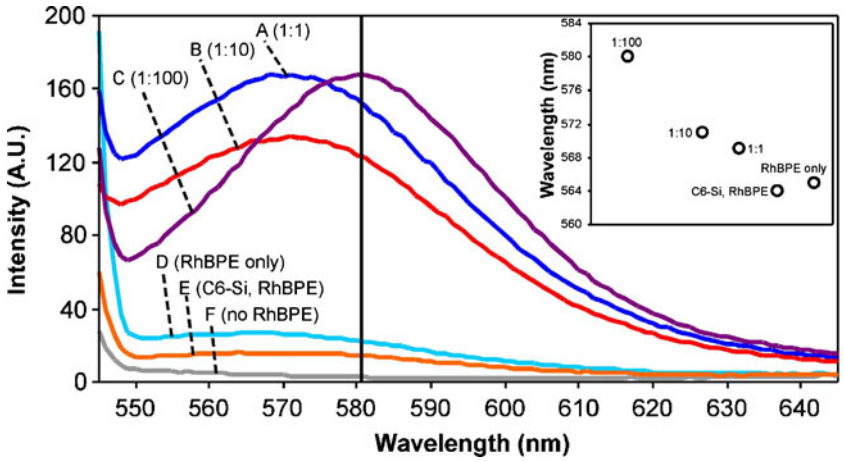

Fig. 4 Fluorescence spectra of glass slides in water. **(A)** 1:1 N3-C6-Si: C6-Si and RhBPE; **(B)** 1:10 N3-C6-Si: C6-Si and RhBPE; **(C)** 1: 100 N3-C6-Si: C6-Si and RhBPE; **(D)** no silane, RhBPE only; **(E)** C6-Si and RhBPE; **(F)** 1:5 N3-C6-Si: C6-Si, no RhBPE. All spectra were obtained with 530 nm excitation. Inset is the λ_{max}^{em} for different samples

prevalent at this moderate surface coverage. The progressive blue shift in λ_{max}^{em} from 580 nm to 570 nm as surface attached dye loading increases is best illustrated in Fig. 3 inset. The small amount of fluorescence from the two control samples (line D and E) is probably due to non-specific RhBEE adsorption onto the glass slides. When compared to the emission spectra of free RhBEE, these blue-shifted emission spectra for surface tethered samples immediately suggest that there are more than just the monomeric species existing in surface attached RhB, especially at sufficiently high surface coverage. Additional evidence of the presence of H-type aggregates can be inferred from the weak emission intensity from the 1:1 and 1:10 samples despite their higher absorbance recorded in Fig. 1. As noted above, this is probably caused by rapid energy transfer from vibronically excited RhB monomers to the surrounding poorly emissive H-type aggregates, quenching the supposedly strong monomer emission and replacing it with the weaker H-type aggregate emission.

Since J-dimers of RhB in solution exhibited a small red shift relative to that of the monomer [42], the blue-shifted emission displayed here is indicative of H-dimer and related aggregates formation. The most stable anti-parallel H-dimer of rhodamine with head-to-tail alignment with respect to the heteroatom is strictly non-emissive [21, 22]. Such anti-parallel H-dimer alignments should be possible for RhB molecules in solution. RhB H-dimer in water is known to exhibit a fairly significant blue shift of ~35 nm and produce a strong absorption band at ~525 nm [10]. Due to constraints imposed by surface tethering, the H-type aggregates in our samples are expected to deviate from the antiparallel orientation. The short tether employed in this study would most likely force the RhB units into less perfectly aligned aggregates. As the H-type aggregates gradually moved away from the most stable anti-parallel configuration, intermolecular separation would increase, causing a smaller exciton splitting and thus a smaller blue shift in both λ_{max}^{abs} and λ_{max}^{em}. The lack of distinctive H-type dimer absorbance at 525 nm and the small blue shifted emission observed here therefore most likely originate from the formation of imperfect H-type aggregates between surface attached RhB, where fluorescence is not entirely forbidden.

The inset in Fig. 3 also shows that the two control samples give the maximum amount of blue shifted emission. Unlike surface attached RhB, non-specifically adsorbed RhBPE are more flexible to adopt more stable H-type aggregates that are closer to the head-to-tail anti-parallel conformations, hence producing the biggest blue shift among all samples.

CB7 Has Strong Affinity Toward Surface Attached RhB

Upon immersion of the dye-tethered slides in 1 mM aqueous CB7, the emission spectra became much more uniform. As demonstrated in Fig. 5, the emission spectra for each sample now resemble that of monomeric RhBEE as well as RhBEE/CB7 complexes in dilute aqueous solution [23]. The reversion back to monomeric type emission upon CB7 addition suggests that CB7 is capable of interacting with surface attached RhB, possibly providing a more uniform chemical environment for RhB by encapsulating the dye inside its hydrophobic cavity. As illustrated in Fig. 5, dye encapsulation inside CB7 should cause a major disruption to the interactions between neighboring RhB molecules, leading to the disintegration of RhB aggregates back to the monomeric species in the form of a RhB/CB7 binary complex (Fig. 6).

The most dilute 1:100 sample (line C in Fig. 5) underwent the smallest change upon CB7 addition, as would be expected from the presumably well-isolated monomeric species. Despite the lack of any spectral shift, the moderate increase in fluorescence intensity does imply the formation of surface attached RhB/CB7 complex. An enhancement factor of less than 2-fold for surface attached RhB upon CB7 binding is close to the 2.5 fold increase determined above from free RhBEE in water.

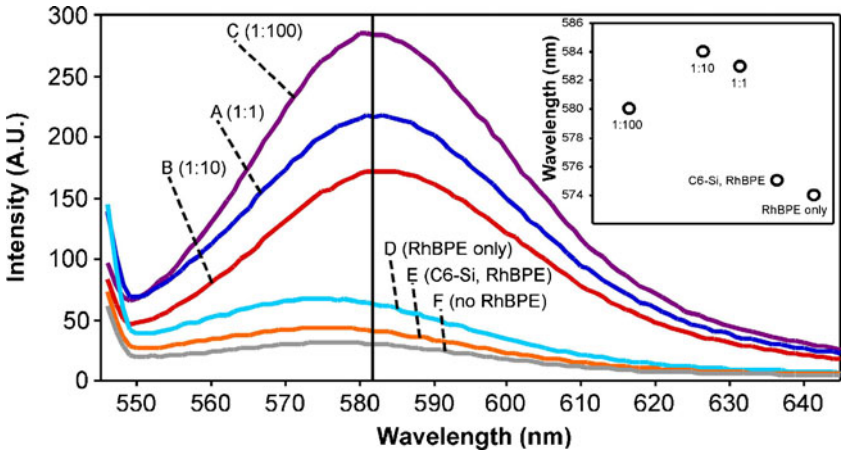

Fig. 5 Fluorescence emission spectra of glass slides in 1 mM aqueous solution of CB7. **(A)** 1:1 N3-C6-Si: C6-Si and RhBPE; **(B)** 1:10 N3-C6-Si: C6-Si and RhBPE; **(C)** 1: 100 N3-C6-Si: C6-Si and RhBPE; **(D)** no silane, RhBPE only; **(E)** C6-Si and RhBPE; **(F)** 1:5 N3-C6-Si: C6-Si, no RhBPE. All spectra were obtained with 530 nm excitation. Inset is the λ_{max}^{em} for different samples

Although CB7 encapsulation can prevent aggregate formation, it may not completely eliminate self quenching between closely packed surface attached RhB/CB7 complexes, thereby resulting in a smaller enhancement. Moreover, the smaller enhancement obtained from surface attached RhB/CB7 may also be due to additional fluorescence quenching by the glass substrate at the glass-water interface [43].

Both 1:1 and 1:10 samples (lines A and B) gave moderate increases in fluorescence intensity accompanied by large bathochromic shift upon CB7 addition, as would be expected from the conversion of H-type aggregate to isolated RhB/CB7 complexes. The bulky CB7 host would have the best opportunity to form complex with all sparsely populated RhB in the 1:100 sample. As RhB surface density increased, the opportunity for complete binding would become progressively more difficult. However, it is worth noting that not all RhB are required to bind to CB7 in order to eliminate aggregate formation. Since both the 1:10 and 1:1 samples gave fairly uniform λ_{max}^{em} near 582 nm, we conclude that enough of the surface attached RhB must have been complexed with CB7 in those samples such that aggregate formation between non-complexed RhB becomes highly unlikely. Similar changes in intensity were observed in the excitation spectra of glass-tethered RhB in water with and without CB7.

We also note the consistently larger blue shift in λ_{max}^{em} seen in the two control samples (lines D and E) relative to all other samples. It appears that CB7 is not as effective in disintegrating aggregates of non-specifically adsorbed RhBPE. Since our synthetic method involves a final cross-linking of the siloxane adlayer after Click attachment of RhBPE to the preliminarily cured adlayer, it is likely that non-specifically adsorbed dye on the glass surface could become covered and physically entrained during the final cross linking step. Since aggregate emission still persists even after rinsing and sonicating the control samples in water, some non-specifically adsorbed RhBPE aggregates were likely to be buried in deep pockets or similar features that prohibited the dyes from leaching out. Meanwhile the relatively large CB7 molecules are also unlikely to have free access to all entrapped dye molecules to disrupt aggregate formation. In the absence of any tethering constraint, these aggregates are arguably of the more stable type, making it more difficult to be disintegrated by CB7 binding. On the other hand, when comparing the inset in Figs. 4 and 5, the λ_{max}^{em} in these two control samples still registered an

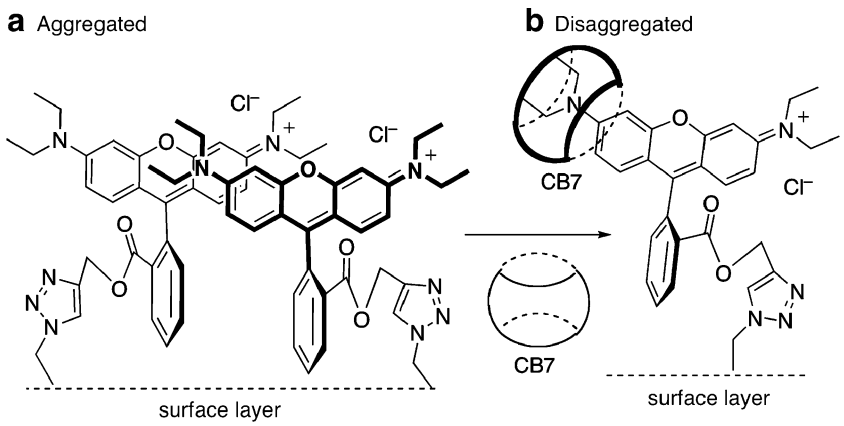

Fig. 6 CB7-induced disaggregation of the surface-bound RhB from a displaced-stacked H-type dimer to the monomeric species

approximately 10 nm bathochromic shift after CB7 addition. This suggests that CB7 is still capable of binding to a small fraction of non-specifically adsorbed RhBPE and weakening RhBPE aggregates interactions. This would lower exciton splitting in the aggregates and thus produce a smaller blue shifted emission.

Conclusions

In summary, we have demonstrated that despite the negative charge on glass surface, CB7 can still effectively bind to surface attached RhB and disrupt aggregate formation. Using a two-step method involving the "Click" triazole formation reaction with a propargyl rhodamine derivative, we were able to prepare samples with varying RhB surface coverage and study the effect of CB7 binding. At low loading, more isolated surface-tethered dyes were formed on the surface and CB7 binding only leads to ~2-fold fluorescence enhancement. On the other hand, aggregate formation at higher RhB surface coverage was evident from the presence of blue-shifted emission. Complexation by CB7 can disrupt aggregate formation and restore the emission back to that of monomeric RhB, consistent with the idea that isolated rhodamine/CB7 inclusion complexes were formed at the expense of H-type RhB aggregates. Given CB7's known ability to enhance the photostability of an inclusion dye, our results suggest that CB7 may find immediate applications in the fabrication of high optical density, high quantum efficiency, and long lasting photovoltaic devices composed of surface-bound dyes**.**

Experimental

Unless otherwise noted, all starting materials, including n-hexyltriethoxysilane, were obtained from commercial suppliers and were used without further purification. The preparation of cucurbit[7]uril (CB7) was adapted from the literature [24]. The preparation of N,N′-bis(2,4,6-trimethyl-pheny)-4,5-dihyro-imidazol-2-ylidine copper (I) bromide [(sIMesCuBr)] was prepared as per the literature [41]. The known 6-bromohexyltriethoxysilane [34] and previously unreported compounds, 6-azidohexyltriethoxysilane **(1)** and rhodamine B propargyl ester **(3)**, were prepared according to the methods presented here. All air- or moisture sensitive reactions were done under an atmosphere of nitrogen. Thin layer chromatography (TLC) analysis was performed using TLC plates (aluminum sheets, 20 cm×20 cm, silica gel 60 F_{254}). Column chromatography was performed using silica gel (230–400 mesh). ^{1}H and ^{13}C spectra were obtained on a 300 MHz NMR spectrometer at ambient temperature. Chemical shifts are expressed in parts per million (δ) using residual solvent protons as an internal standard (1.94 for CD_3CN). Coupling constants, *J*, are reported in Hertz (Hz), and splitting patterns are designated as s (singlet), d (doublet), t (triplet), q (quartet), and m (multiplet).

Glass Substrate Preparation Piranha solution (70:30, 98% H_2SO_4: 30% H_2O_2) was prepared by the slow addition of cold (0 °C–4 °C) 30% H_2O_2 to a glass beaker containing cold (0 °C–4 °C) 98% H_2SO_4. The mixture was stirred in an ice bath for 30 min to facilitate mixing and cooling. **Warning:** *Extreme care should be taken when preparing and using the "piranha" solution as the solution can detonate when in contact with organic compounds.* Cold 30% H_2O_2 and 98% H_2SO_4 was used to prevent frothing due to heat generated during mixing. Float glass cuvette slides (7 mm×50 mm×0.7 mm) were placed in borosilicate glass test tubes (13 mm×100 mm), one per test tube. Piranha solution was added to the test tubes using a glass Pasteur pipette so that each glass slide was completely submerged. The glass slides were allowed to soak in the piranha solution for 12 h at room temperature. After 12 h, the piranha solution was pipetted out of the test tubes into a glass storage container. The glass slides were rinsed in the test tubes by filling the test tubes with Millipore water and subsequently transferring the rinse water from the test tubes into a separate glass storage container. This rinse procedure with Millipore water was repeated two additional times. After the third and final rinse, the test tubes were filled with Millipore water so that the glass slides were completely submerged. The test tubes were covered with plastic wrap and stored at room temperature. The used piranha solution should be transferred from the glass storage container into a properly labeled clean glass bottle in an isolated and properly labeled laboratory fume hood. The used rinse water can be transferred and stored into the same glass bottle used to store the used piranha solution.

Formation of Mixed Silane Layers on Glass Substrate Freshly cleaned glass slides were placed in polystyrene cuvettes and immersed for 2 h at room temperature in silane solutions (3.5 mL) prepared by dissolving the desired ratio of 6-azidohexyltriethoxysilane and diluent n-hexyltriethoxysilane in dry acetonitrile in the presence of glacial acetic acid (5 mM). The total silane concentration was fixed at 10 mM. Following the silane treatment the glass slides were removed from the polystyrene cuvettes, placed in glass test tubes (13 mm×100 mm) and cured in a vacuum oven at 60 °C for 4 h.

Surface Coupling by Cu(I) Catalyzed Azide-Alkyne 1,3-Dipolar Cycloaddition Following the initial heat cure, the silane treated slides were placed in polystyrene cuvettes and immersed for 8 h in a mixture (3.5 mL) of *tert*-butyl alcohol:

Millipore water (3:1) containing rhodamine B propargyl ester (5 mM) and sIMesCuBr (10 mol%) at room temperature in the dark. The treated glass slides were removed from the dye coupling solutions, dip rinsed three times in 95% ethanol and dried by centrifugation. The dried glass slides were transferred to clean glass test tubes and cured in a vacuum oven at 90 °C for 4 h. The heat-cured glass slides were then dip-rinsed three times in a mixture of absolute ethanol:water (1:1). The rinsed glass slides were transferred to clean test tubes and immersed in a solution of absolute ethanol: Millipore water (1:1) for 16 hours at room temperature in the dark. After 16 hours, the slides were transferred to fresh glass test tubes and dried by centrifugation.

Absorption Measurements Absorption measurements were performed using a UV-Vis scanning spectrophotometer (Shimadzu UV-2101PC) using disposable polystyrene cuvettes of 10.0 mm path for the samples measured in Millipore water and aqueous CB7 (1 mM). The baseline was recorded with water in the reference cuvette using glass slides treated with only n-hexyltriethoxysilane. No cuvette was used for the glass slides measured in air in the absence of solvent. All measurements were performed at ambient temperature. The glass slides were treated with varying mixtures of n-hexyltriethoxysilane: 6-azidohexyltriethoxysilane followed by subsequent treatment with rhodamine B propargyl ester on each side of the glass slides; therefore, all absorbance spectra are from two surfaces.

Fluorescence Measurements Steady-state measurements were performed using a spectrofluorophotometer (Shimadzu RF-3101PC), equipped with a Xenon lamp of 150 W as the excitation source, using disposable polystyrene cuvettes of 10.0 mm path for the samples measured in Millipore water and aqueous CB7 (1 mM). Fluorescence emission spectra were collected using an excitation wavelength of 530 nm. The slit width was adjusted to 10 for all measurements. All measurements were performed at ambient temperature. The glass slides were treated with varying mixtures of n-hexyltriethoxysilane:6-azidohexyltriethoxysilane followed by subsequent treatment with rhodamine B propargyl ester on each side of the glass slides; therefore, all fluorescence spectra are from two surfaces.

Synthesis of 6-Bromohexyltriethoxysilane A mixture of 6-bromo-1-hexene (1.00 g, 6.13 mmol), triethoxysilane (1.51 g, 0.190 mmol) and 0.1 M Karstedt catalyst in xylenes (1 mL) was stirred under nitrogen at 80 °C for 72 h. The crude reaction mixture was distilled under reduced pressure (0.1 mm Hg) at 88 °C to give **5.1** (1.62 g, 4.94 mmol, 81%) as a transparent colorless liquid: ^{1}H NMR (300 MHz, CD_3CN): δ 3.77 (q, J=6.9 Hz, 6 H), 3.46 (t, J=6.8 Hz, 2 H), 1.82 (m, 2 H), 1.41 (m, 6 H), 1.17 (t, J=6.9, 9 H), 0.58 (t, J=6.3, 2 H).

^{1}H NMR Spectrum (300 MHz, CD_3CN) of 6-Bromohexyltriethoxysilane

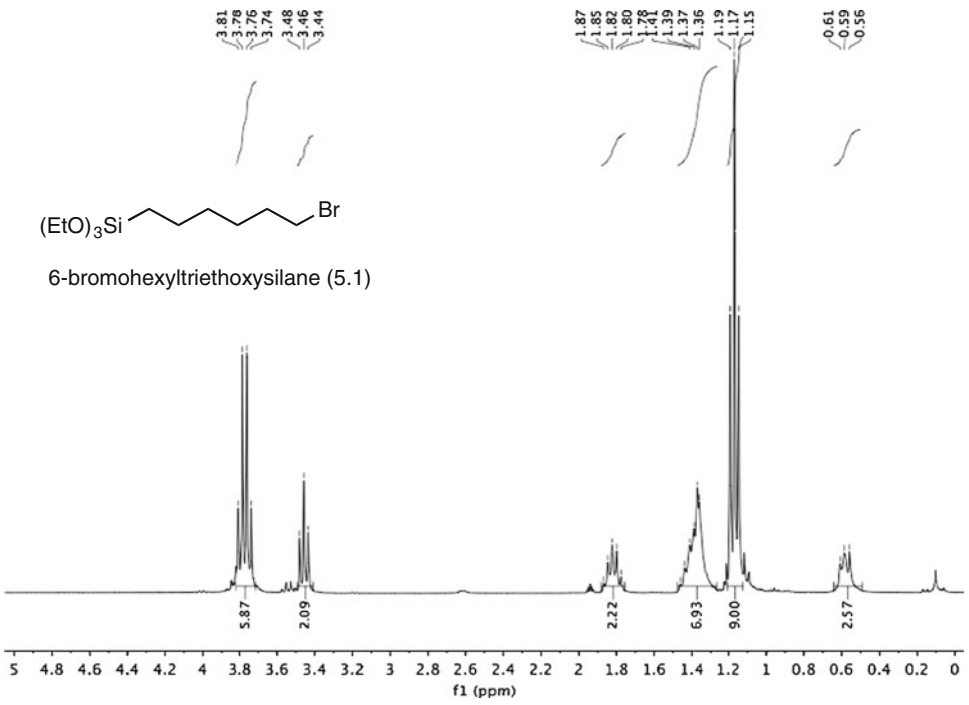

Synthesis of 6-Azidohexyltriethyoxysilane (1) The 6-bromohexyltriethoxysilane (1.11 g, 3.40 mmol) was dissolved in DMSO (55 mL). To this solution was added NaN_3 (0.243 g, 3.74 mmol) and the mixture was stirred under nitrogen at room temperature for 48 h. The reaction was quenched with H_2O (50 mL) and stirred for 15 min. The aqueous mixture was extracted with Et_2O (3×25 mL). The combined Et_2O extracts were washed with brine (25 mL) and H_2O (2×25 mL). The organic layer was dried (Na_2SO_4), and concentrated under reduced pressure to give **5.2** (0.723 g, 4.18, mmol, 74%) as a transparent colorless liquid: ^{1}H NMR (300 MHz, CD_3CN): δ 3.79 (q, J=7.0 Hz, 6 H), 3.22 (t, J=6.9 Hz, 2 H), 1.56 (m, 2 H), 1.37 (m, 6 H), 1.20 (t, J=7.0 Hz, 9 H), 0.60 (t, J=7.7 Hz, 2 H).

^{1}H NMR Spectrum (300 MHz, CD_3CN) of 6-Azidohexyltriethoxysilane (1)

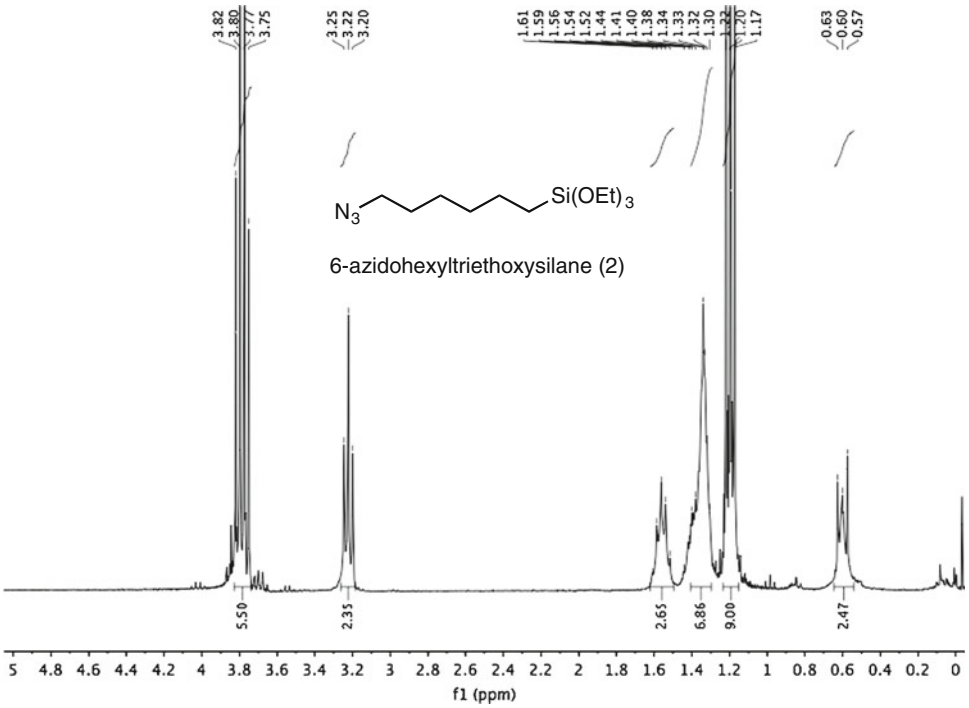

Synthesis of Rhodamine B Propargyl Ester (3) A mixture of rhodamine B (4.00 g, 8.35 mmol), methylene chloride (150 mL), 1,3-dicyclohexylcarbodiimide (2.15 g, 10.4 mmol), propargyl alcohol (2.34 g, 41.8 mmol), and 4-dimethylaminopyridine (0.102 g, 0.830 mmol) was stirred under nitrogen at room temperature for 96 h. The crude dark pink filtrate was collected by vacuum filtration and concentrated at room temperature under reduced pressure. A portion of the crude product (0.447 g) was purified by silica gel column chromatography with methanol/chloroform, 9:1 to elute unreacted rhodamine B followed by methanol/chloroform/glacial acetic acid, 90:10:1 to give **5.3** (0.371 g, 0.720 mmol, 83%) as a purple/red waxy solid: ^{1}H NMR (300 MHz, CD_3CN): δ 8.28 (m, 1 H), 7.84 (m, 2 H), 7.40 (m, 1 H), 7.06 (d, J=9.5 Hz, 2 H), 6.93 (dd, J=2.5, 9.5 Hz, 2 H),

6.84 (d, J=2.5 Hz, 2 H), 4.59 (d, J=2.5 Hz, 2 H), 3.61 (q, J=7.1 Hz, 8 H), 2.64 (t, J=2.5 Hz, 1 H), 1.24 (t, J=7.1 Hz, 12 H).

^{1}H NMR Spectrum (300 MHz, CD_3CN) of Rhodamine B Propargyl Ester (3)

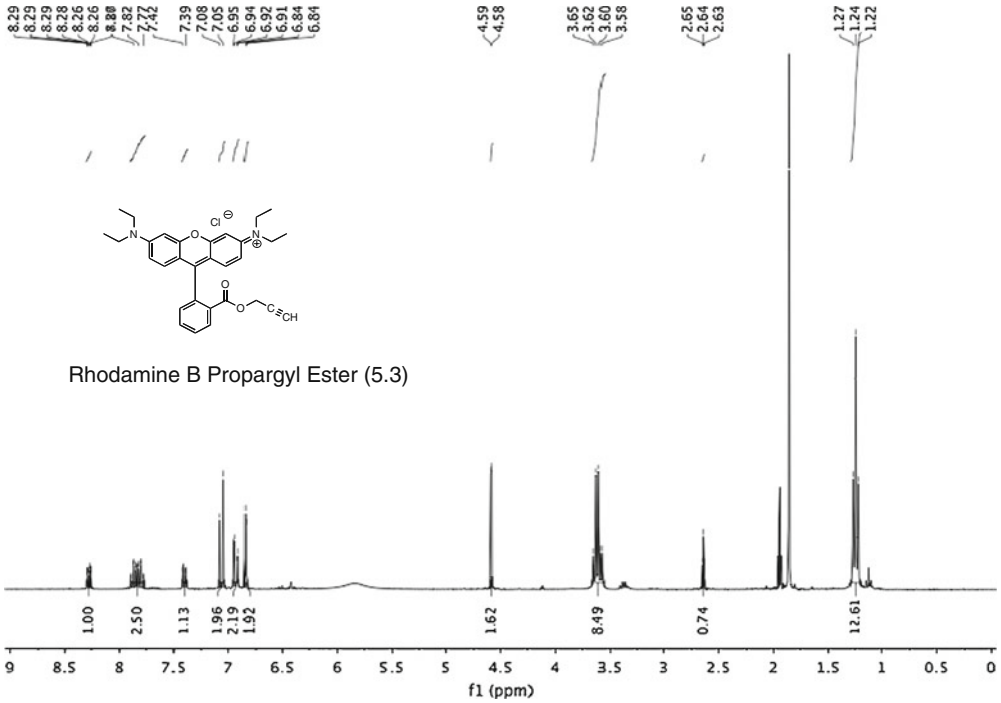

Acknowledgment The support of NSF (DMR-0805233 to RLH, CHE-0442151 to WTY) is acknowledged as well as a DoEd GAANN fellowship to JLM.

References

1. Ooyama Y, Harima Y (2009) Eur J Org Chem 2009:2903
2. Gratzel M (2005) Inorg Chem 44:6841
3. de Schryver FC, Vosch T, Cotlet M, van der Auweraer M, Müllen K, Hofkens J (2005) Acc Chem Res 38:514
4. Tietz C, Jelezko F, Gerken U, Schuler S, Schubert A, Rogl H, Wrachtrup J (2001) Biophys J 81:556
5. Zhang Y-H, Gao Z-X, Zhong C-L, Zhou H-B, Chen L, Wu W-M, Peng X-J, Yao Z-J (2007) Tetrahedron 63:6813
6. Kálai T, Hideg K (2006) Tetrahedron 62:10352
7. Chang PV, Prescher JA, Hangauer MJ, Bertozzi CR (2007) J Am Chem Soc 129:8400
8. Nau WM, Mohanty J (2005) Int J Photoenergy 7:717
9. Meier JL, Mercer AC, Rivera H, Burkart MD (2006) J Am Chem Soc 128:12174
10. Selwyn JE, Steinfeld JI (1972) J Phys Chem 76:762
11. Rohatgi KK, Singhal GS (1966) J Phys Chem 70:1695
12. Martyn TA, Moore JL, Halterman RL, Yip WT (2007) J Am Chem Soc 129:10338
13. Gilliland JW, Yokoyama K, Yip WT (2005) Chem Mater 17:6702
14. Chambers RW, Kajiwara T, Kearns DR (1974) J Phys Chem 78:380
15. Abad S, Kluciar M, Miranda MA, Pischel U (2005) J Org Chem 70:10565
16. Guo X, Zhang D, Zhou Y, Zhu D (2003) J Org Chem 68:5681
17. Mori T, Ko YH, Kim K, Inoue Y (2006) J Org Chem 71:3232
18. Bujdak J, Iyi N (2006) J Phys Chem B 110:2180
19. Gutierrez MC, Hortiguela MJ, Ferrer ML, del Monte F (2007) Langmuir 23:2175
20. Avnir D, Levy D, Reisfeld R (1984) J Phys Chem 88:5956
21. Ilich P, Mishra PK, Macura S, Burghardt TP (1996) Spectrochim Acta A 52:1323

22. Gal ME, Kelly GR, Kurucsev T (1973) J Chem Soc, Faraday Trans 2(69):395
23. Halterman RL, Moore JL, Mannel LM (2008) J Org Chem 73:3266
24. Day A, Arnold AP, Blanch RJ, Snushall B (2001) J Org Chem 66:8094
25. Kim J, Jung I, Kim S, Lee E, Kang J, Sakamoto S, Yamaguchi K, Kim K (2000) J Am Chem Soc 122:540
26. Lagona J, Mukhopadhyay P, Chakrabarti S, Isaacs L (2005) Angew Chem Int Ed 44:4844
27. Fiorilli S, Onida B, Barolo C, Viscardi G, Brunel D, Garrone E (2007) Langmuir 23:2261
28. See for instance, Invitrogen's "Molecular Probes The Handbook–A guide to fluorescent probes and labeling technologies" http://www.invitrogen.com/site/us/en/home/References/Molecular-Probes-The-Handbook.html
29. Wang R, Yuan L, Macartney DH (2005) Chem Commun 41:5867
30. Ong W, Gomez-Kaifer M, Kaifer AE (2002) Org Lett 4:1791
31. Yuan L, Wang R, Macartney DH (2007) J Org Chem 72:4539
32. Moon K, Kaifer AE (2004) Org Lett 6:185
33. Collman JP, Devaraj NK, Chidsey CED (2004) Langmuir 20:1051
34. Pichon BP, Wong Chi Man M, Bied C, Moreau JJE (2006) J Organomet Chem 691:1126
35. Hassner A, Alexanian V (1978) Tetrahedron Lett 46:4475
36. MacBeath G, Koehler AN, Schreiber SL (1999) J Am Chem Soc 121:7967
37. Gao L, Liu S (2004) Anal Chem 76:7179
38. Lenhart JL, van Zanten JH, Dunkers JP, Zimba CG, James CA, Pollack SK, Parnas RS (2000) J Colloid Interf Sci 221:75
39. Bock VD, Hiemstra H, van Maarseveen JH (2006) Eur J Org Chem 2006:51
40. Rostovtsev VV, Green LG, Fokin VV, Sharpless KB (2002) Angew Chem Int Ed 41:2596
41. DÌez-Gonzalez S, Correa A, Cavallo L, Nolan SP (2006) Chem Eur J 12:7558
42. del Monte F, Levy D (1998) J Phys Chem B 102:8036
43. Lee M, Kim J, Tang J, Hochstrasser RM (2002) Chem Phys Lett 359:412